Employment of the Multiple Endmember Spectral Mixture Analysis (MESMA) Method in Mineral Analysis

OSMAR ABÍLIO DE CARVALHO JÚNIOR[1]
RENATO FONTES GUIMARÃES[1]

[1]Departamento de Geografia - Universidade de Brasília (UnB)- Campus Universitário Darcy Ribeiro, Asa Norte, 70910-900, Brasília, DF, Brazil
osmana@tba.com.br

Abstract: In the analysis of a spectral mixture, the Spectral Mixture Analysis (SMA) method presents many errors because it is hard to adjust the endmembers in the image with the elements really in each pixel. A method proposed to eliminate that source of mistakes is the Multiple Endmember Spectral Mixture Analysis (MESMA), which defines through the root mean square the best association of spectral mixture that describes each pixel. A routine was developed in IDL, which accomplishes that comparison of the models of mixtures defined for each pixel the most appropriate. This method was tested in the Niquelândia (Brazil) mine and showed excellent results being in agreement with the field.

Keywords: Spectral mixture, MESMA, imaging spectroscopy.

1 Introduction

Spectral Mixture Analysis (SMA) uses the multiple linear regression to define the endmembers abundance in the image (Smith & Adams, 1985). The main source of errors of SMA is that it considers all the pixels as a mixture of an unique initial group of endmembers. This way, the errors are (Sabol *et al.*, 1992):

a) Spectral variability of model components, and

b) Absence of modeled components.

The ideal condition of endmembers is difficult to obtain. Both insufficiency and excess of final members cause errors in SMA. To correct that kind of error it was proposed a new method that establishes for each pixel the best mixture model (Smith *et al*., 1992; Sabol *et al*., 1992; Roberts *et al*., 1992). The evolution of this proposal was the development of the Multiple Endmember Spectral Mixture Analysis (MESMA) (Roberts *et al*., 1998a). The MESMA differs from SMA because allows the number and the quantity of endmembers vary pixel by pixel in the image.

The MESMA adopts as the best model the one that has smaller root mean square (rms) error when compared to the spectral curve of the pixel (Okin *et al*., 1998). The MESMA has been applied in the mapping of different areas (Painter *et al*., 1996, 1998a, 1998b, Gardner, 1997; Roberts *et al*., 1998a, 1998b, Okin *et al*., 1998, 1999a). However, Roberts *et al*. (1998a) points to the necessity of additional research.

The computational effort is a problem to apply this method (Okin *et al*., 1999b). The amount of endmembers increases as much as the possible combinations increasing the computational effort. To avoid the unnecessary use of models, it can be done a previous image segmentation for

the use of spectral classifiers, for instance, the Spectral Correlation Mapper (SCM) method (Carvalho & Meneses, 2000).

2. The employment of the MESMA for mineral analysis

The MESMA was applied to the AVIRIS subscene of Niquelândia, Brazil, that inclues a nickel lateritic mine. The main minerals present in the weathering profile are: pimelite/saponite, goethite, hematite and kaolinite.

To decrease the computational effort was applied the SCM that accomplishes a pre-classification of the mineral. A program in IDL language was developed to identify the best-fit models considering the minor rms error. The program disrespects model with negative values. The program presents as outputs: a) weighting coefficients images of each endmember, b) the rms image and c) an image with the most appropriate model to each pixel. The spectral range delineation of the minerals absorption features (0,43μm to 0,75 μm and 2,09 μm to 2,38 μm) allows a best-fit model. The MESMA algorithm was applied on spectra with and without the continuum removal.

a) Image

The weighting coefficient images related to the minerals from Niquelândia mine corresponds to the field observation (Figure 1). The clearest areas correspond to the major percentage of the mineral. A profile from the base to top mine is well characterized by the image. Pimelite-saponite and goethite constitute the base profile and, upward, is observed an increase of hematite and kaolinite. The RMS image shows the major errors in pimelite-saponite areas, probably due to the worse fit in the visible range (Figure 2).

Only six models were selected (Figure 3). The models ware coherent for most of the area. However some errors were observed, i.e. the model 2 on the mine top is wrong due to pimelite presence. Although, it doesn't compromise the method because of low values of pimelite.

b) Continuum-removed image

The weighting coefficient on the continuum-removed spectra corresponds to the normalized absorption band area. That index is equivalent to the scale coefficient (normalized absorption band depth) intensively used in the mineral abundance analysis. Figure 4 demonstrates the high correlation between those two factors considering the kaolinite feature.

A similarity exists among the images of the minerals with and without continuum removal (Figure 5). However, in that procedure only four mixture models are detected (Figure 6). The best-fit model is the one that contains all of them. That fact is due to two factors deriving from continuum removal: a) detection capacity of minerals in minor quantity, b) greater susceptibility to noise interference (Carvalho *et al*., 2000). In spite of the best-fit model contain the four minerals, it was observed that the percentage of some of them is minimum. This way, the hematite detected in basal zone of the mine has the lowest values (Figure 7).

RMS image demonstrates that the models with worse fittings were concentrated in the limits of the mine where begins to appear the interference of the vegetation (Figure 7). The rms in the classification with the continuum removal is much smaller than the obtained without the continuum removal what demonstrates a better fit. It is observed that the error from the pimelite-saponite mineral decrease.

a) Pimelite - Saponite

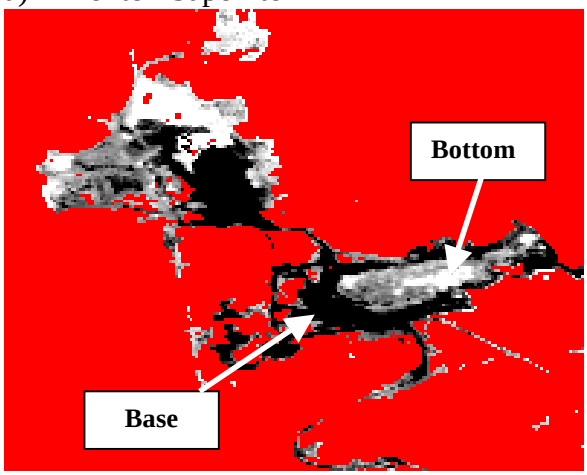

b) Goethite

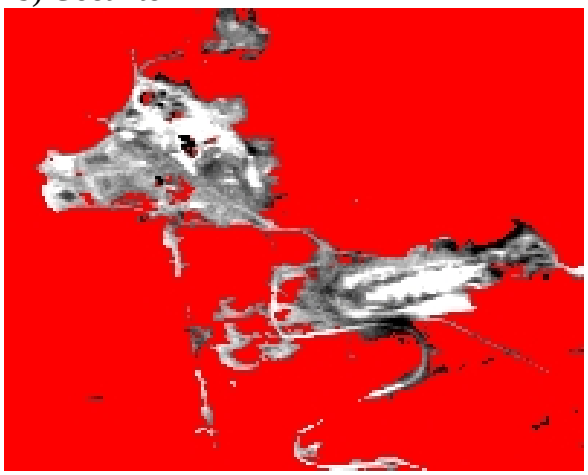

c) Hematite

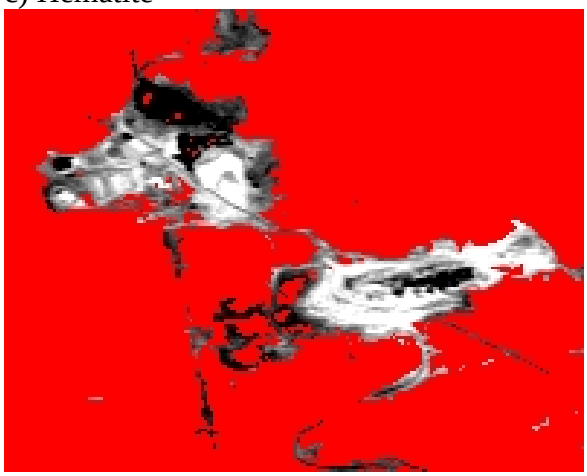

d) Kaolinite

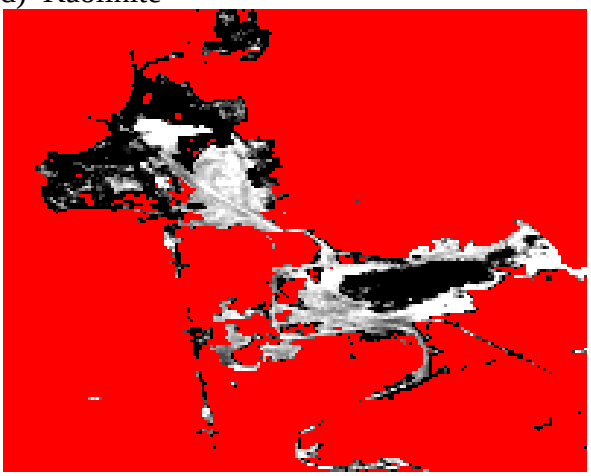

Figure 1 - Mineral images of the MESMA methods: a) pimelite-saponite, b) goethite, c) hematite, and d) kaolinite

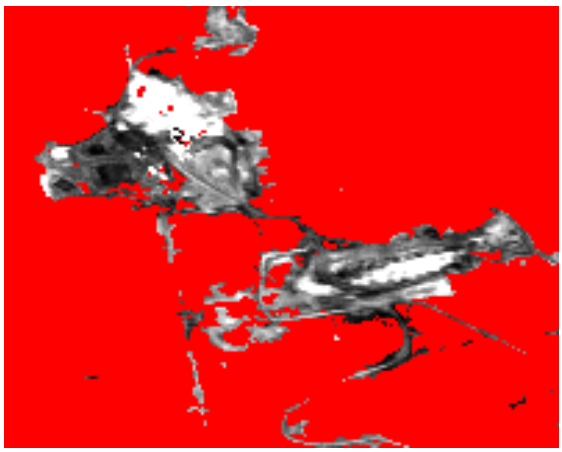

Figure 2 – The rms image

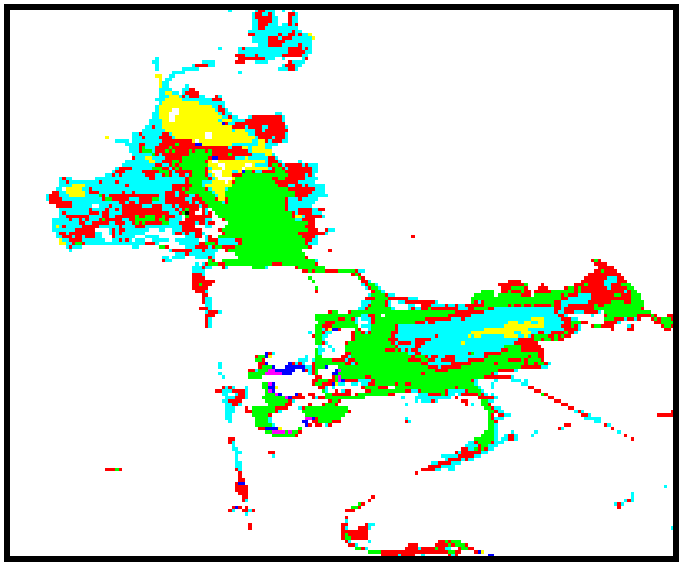

1 - pimelite-saponite and goethite

2 - pimelite-saponite, goethite and hematite

3 - pimelite-saponite, kaolinite, goethite and hematite.

4 - kaolinite, goethite and hematite

5 - pimelite-saponite, kaolinite and goethite

6 - kaolinite and goethite

Figure 3 – Mixture models image

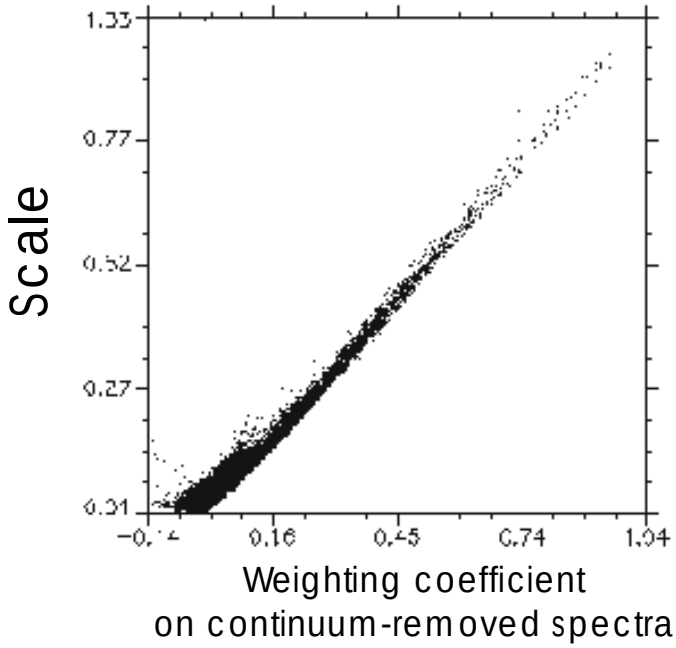

Figure 4 - Relationship of the scale coefficient with the weighting coefficient on continuum-removed spectra (normalized absorption band area).

a) Pimelite - Saponite

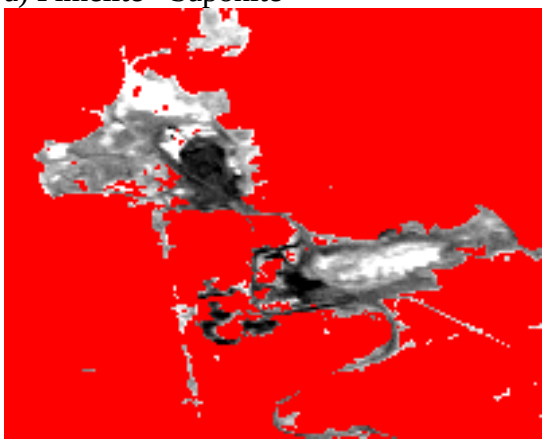

b) Goethite

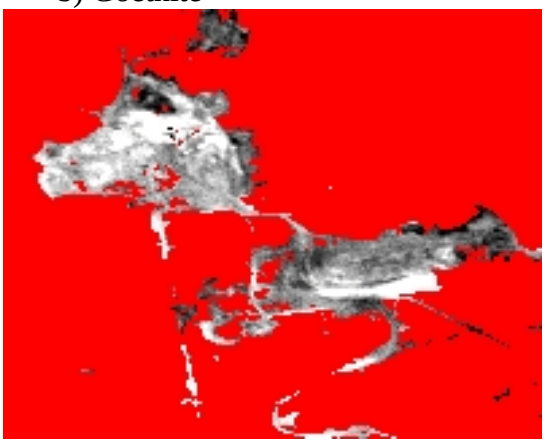

c) Hematite

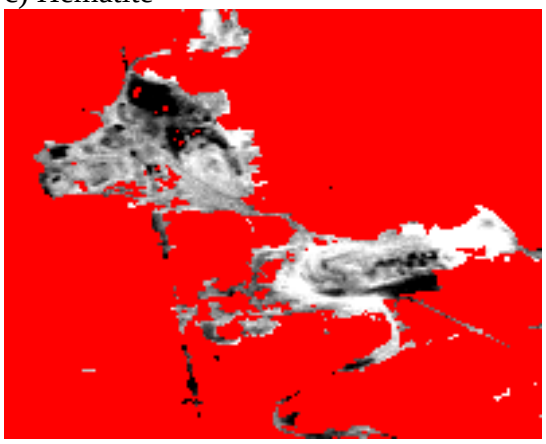

d) Kaolinite

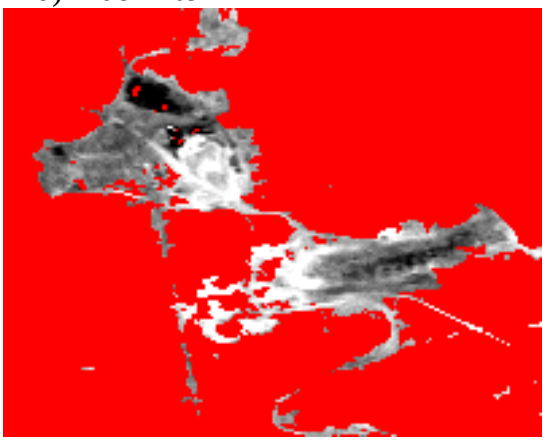

Figure 5 - Mineral images of the MESMA method considering continuum removal spectra: a) pimelite, b) kaolinite, c) goethite, and d) hematite

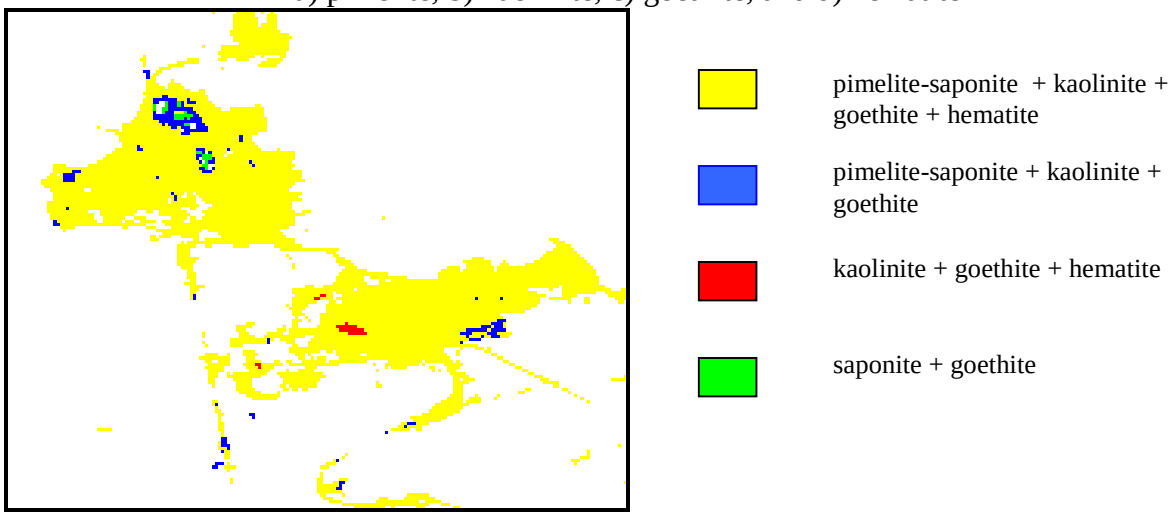

Figure 6 –Disposition of the models selected by the MESMA considering continuum-removed spectra.

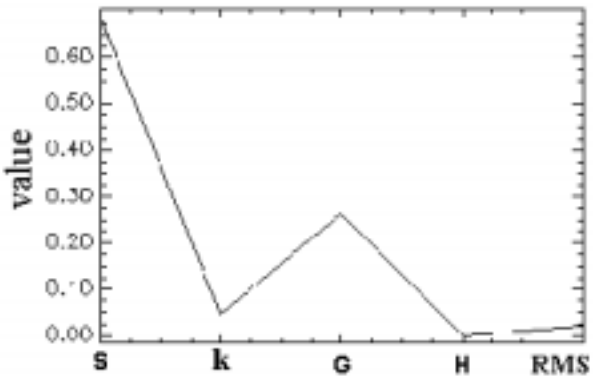

Figure 7 – Abundance distribution for a pixel placed in the zone garnieritic. S = saponite, C=kaolinite, G = goethite, H=hematite and RMS.

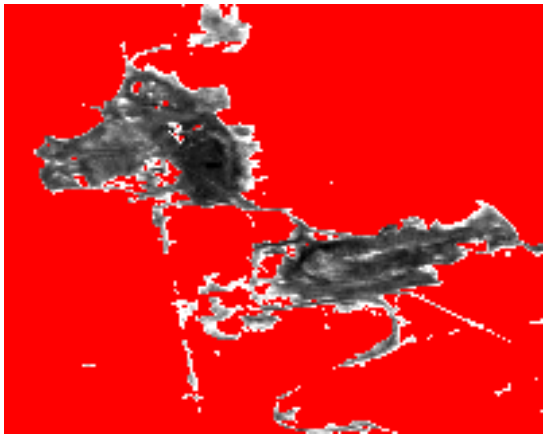

Figure 8 – RMS image of the MESMA from the continuum-removed spectra.

3 - Conclusion

The main conclusions are:

- MESMA method is an improvement of the SMA method because it allows identifying the best model for each pixel.
- The use of the spectral classifier SCM allows to select areas of interest decreasing the computational time. In the use of SCM the mineral occurrence can be overestimated because the MESMA define the best model.
- The delimitation of the spectrum for the absorption features of the existent minerals allows a better model adjustment. That procedure also allows decreasing the computational time.
- The use of the continuum removal spectra allows obtaining weights compatible to the scale coefficient, which is widely used in the mineral analysis.
- In the study area the continuum removal increased the number of models with the four minerals in the analysis due to: a) the larger detection capacity in a smaller abundance of minerals b) great susceptibility to noise interference. However, many minerals present very low concentrations.
- MESMA is a complete method because as allows identifying the areas of occurrence of the minerals as supplies indicators of its abundance.

References

Carvalho Jr., O. A. & Meneses, P. R., 2000, Spectral Correlation Mapper (SCM): An Improving Spectral Angle Mapper (SAM). *The Ninth JPL Airborne Earth Science Workshop*. http: //makalu.jpl.nasa.gov/docs/workshops/toc. htm

Carvalho Jr., O. A., Carvalho, A. P. F., & Meneses, P. R., 2000, An Approach to Hyperspectal Image Classification Based on Linear Regression. *The Ninth JPL Airborne Earth Science Workshop*. http: //makalu.jpl.nasa.gov/docs/workshops/toc. htm

Gardner, M., 1997, Mapping Chaparral with AVIRIS Using Advanced Remote Sensing Techniques, Master of Arts thesis: Department of Geography, University of California, Santa Barbara, CA.

Okin, G. S.; Okin, W. J.; Roberts, D. A.; Murray, B., 1998, Multiple Endmember Spectral Mixure Analysis: Application to an Arid/Semi-arid Landscape. *Summaries of the 7th JPL Airborne Earth Science Workshop*, JPL Publication 97-21 v.1, pp. 291-299.

Okin, G. S.; Siegel, H.; Collier, J.; Miller, G. D., Okin, W. J.; Roberts, D. A., Murray B., Curkendall, D. W.; Painter, T. H., 1999b, The Supercomputing Vizualization Workbench for Analysis and Classification of Imaging Spectrometer Data. *Summaries of the 8th JPL Airborne Earth Science Workshop*, JPL Publication 99-17 v.1, pp. 317-322.

Okin, W. J.; Okin, G. S.; Roberts, D. A; Murray B., 1999a, Multiple Endmember Spectral Mixture Analysis: Endmember Choice in an Arid Shrubland, *Summaries of the 8th JPL Airborne Earth Science Workshop*, JPL Publication 99-17 v.1, pp. 323-331.

Painter, T. H., Roberts, D. A.; Dozier J.; Green, R. O., 1998a, Automated Subpixel Snow Parameter Mapping with AVIRIS Data. *Summaries of the 7th JPL Airborne Earth Science Workshop*, JPL Publication 97-21 v.1, pp. 301-307.

Painter, T. H., Roberts, D. A.; Green, R. O. & Dozier J.; 1998b, The Effect of Grain Size on Spectral Mixture Analysis of Snow-Covered Areas from AVIRIS Data. *Remote Sens. Environ.* 65:320-332.

Painter, T. H., Roberts, D. A.; Green, R. O., Dozier J.; 1996, Subpixel Snow-Covered Area and Sow Grain Size from Mixture Analysis with AVIRIS Data. *Summaries of the 6th Annual JPL Airborne Earth Science Workshop*, JPL Publication 96-4 v.1.

Roberts, D. A., Smith, M. O., Sabol, D. E., Adams, J. B. & Ustin, S., 1992, Mapping the Spectral Variability in Photosynthetic and Non-photosynthetic Vegetation, Soils and Shade Using AVIRIS. *Summaries of the 3rd Annual JPL Airborne Geoscience Workshop*, JPL Publication 92-14, v.1, pp. 38-40.

Roberts, D. A.; Gardner, M.; Church R., Ustin, S. Scheer, G. & Green, R. O., 1998a, Mapping Chaparral in the Santa Monica Mountains using multiple endmember spectral mixture models. *Remote Sens. Environ*. 65:267-279.

Roberts, D. A.; Gardner, M.; Regelbrugge, J.; Pedreros, D.; Ustin, S. L., 1998b, Mapping the Distribution of Wildfire Fuels Using AVIRIS in the Santa Monica Mountains. *Summaries of the 7th JPL Airborne Visible/Infrared Imaging Spectrometer (AVIRIS) Workshop*, JPL Publication 97-21 v.1, pp. 345-352.

Sabol D. E. Jr., Adams J. B. & Smith M. O. 1992, Quantitative Subpixel Spectral of Targets in Multiespectral Images, *J. Geophys. Res*., 97, 2.659-2.672.

Smith, M. O. & Adams, J. B. 1985, Interpretation of AIS images of Cuprite, Nevada, using constraints of spectral mixtures. In: Proc. Airborne Imaging Spectrometer Data Analysis Workshop, JPL Publication 85-41, pp. 62-68.

Smith, M. O., Adams J. B., Ustin S. L. & Roberts, D. A., 1992, Using endmembers in AVIRIS images to estimate changes in vegetative biomass. *Summaries of the 4th Annual JPL Airborne Geoscience Workshop*, JPL Publication 92-14, v.1, pp. 69-71.